American College of Neuropsychopharmacology

www.nature.com/npp

ARTICLE

Check for updates

Adolescent alcohol use is linked to disruptions in age-appropriate cortical thinning: an unsupervised machine learning approach

Delin Sun[1,2,3], Viraj R. Adduru[1,2,4], Rachel D. Phillips[1,2], Heather C. Bouchard[1,2], Aristeidis Sotiras[5], Andrew M. Michael[1,4], Fiona C. Baker[6], Susan F. Tapert[7], Sandra A. Brown[7], Duncan B. Clark[8], David Goldston[9], Kate B. Nooner[9], Bonnie J. Nagel[10], Wesley K. Thompson[7], Michael D. De Bellis[1,11] and Rajendra A. Morey[1,2,11,12]✉

Cortical thickness changes dramatically during development and is associated with adolescent drinking. However, previous findings have been inconsistent and limited by region-of-interest approaches that are underpowered because they do not conform to the underlying spatially heterogeneous effects of alcohol. In this study, adolescents ($n = 657$; 12–22 years at baseline) from the National Consortium on Alcohol and Neurodevelopment in Adolescence (NCANDA) study who endorsed little to no alcohol use at baseline were assessed with structural magnetic resonance imaging and followed longitudinally at four yearly intervals. Seven unique spatial patterns of covarying cortical thickness were obtained from the baseline scans by applying an unsupervised machine learning method called non-negative matrix factorization (NMF). The cortical thickness maps of all participants' longitudinal scans were projected onto vertex-level cortical patterns to obtain participant-specific coefficients for each pattern. Linear mixed-effects models were fit to each pattern to investigate longitudinal effects of alcohol consumption on cortical thickness. We found in six NMF-derived cortical thickness patterns, the longitudinal rate of decline in no/low drinkers was similar for all age cohorts. Among moderate drinkers the decline was faster in the younger adolescent cohort and slower in the older cohort. Among heavy drinkers the decline was fastest in the younger cohort and slowest in the older cohort. The findings suggested that unsupervised machine learning successfully delineated spatially coordinated patterns of vertex-level cortical thickness variation that are unconstrained by neuroanatomical features. Age-appropriate cortical thinning is more rapid in younger adolescent drinkers and slower in older adolescent drinkers, an effect that is strongest among heavy drinkers.

Neuropsychopharmacology (2023) 48:317–326; https://doi.org/10.1038/s41386-022-01457-4

INTRODUCTION

Neuromaturation during childhood and adolescence undergoes a dramatic transformation of cortical gray-matter thickness and volume. Gray matter volume peaks before the teen years and then declines into adulthood as underutilized connections between neurons are pruned [1–3]. Widespread differences in brain morphometry are observed in adolescent drinkers [4, 5]. Heavy adolescent alcohol use [6] is associated with faster cortical grey matter decline, possibly related to vulnerability during adolescent development [4]. However, slower grey matter thinning is also hypothesized on the premise that alcohol disrupts the process of pruning [6].

Alcohol is the most commonly misused substance with 24% of adolescents reporting consumption by 8th grade and 59% before the end of high school [7]. An alarming number of drinks are consumed by adolescents [8] who drink less frequently and overall consume less than adults, but are more likely to binge drink [9]. Binge drinking prevalence increases between 12–25 years [8] with 14% of 12th graders binging every two weeks [7].

Hypothesis-driven region-of-interest (ROI) analyses have identified lower cortical thickness in the frontal, temporal, parietal, occipital, and cingulate cortices [2, 10, 11] of adolescent binge drinkers compared to light or non-drinking peers [12], an effect that was further amplified among younger adolescents [13, 14]. By contrast, competing findings of higher cortical thickness in the frontal, parietal, temporal, and occipital regions [13, 15] have been reported. Previous studies have tested mean cortical thickness in anatomically defined ROIs. However, the patterns of brain maturation and the disrupted patterns in cortical thickness that are associated with binge drinking, do not necessarily follow neuroanatomical boundaries along prescribed gyral and sulcal features.

[1]Duke-UNC Brain Imaging and Analysis Center, Duke University, Durham, NC, USA. [2]VA Mid-Atlantic MIRECC, Durham VA Medical Center, Durham VA, Durham, NC, USA. [3]Department of Psychology, The Education University of Hong Kong, Hong Kong, China. [4]Chester F. Carlson Center for Imaging Sciences, Rochester Institute of Technology, Rochester, NY, USA. [5]Department of Radiology and Institute for Informatics, University of Washington, St Louis, MO, USA. [6]Biosciences Division, SRI International, Menlo Park, CA, USA. [7]Department of Psychiatry, University of California San Diego, La Jolla, CA, USA. [8]Department of Psychiatry, University of Pittsburgh, Pittsburgh, PA, USA. [9]Department of Psychology, University of North Carolina Wilmington, Wilmington, NC, USA. [10]Departments of Psychiatry and Behavioral Neuroscience, Oregon Health & Science University, Portland, OR, USA. [11]Department of Psychiatry and Behavioral Sciences, Duke University, Durham, NC, USA. [12]Center for Cognitive Neuroscience, Duke University, Durham, NC, USA. ✉email: rajendra.morey@duke.edu

Received: 13 June 2022 Revised: 16 August 2022 Accepted: 6 September 2022
Published online: 8 October 2022

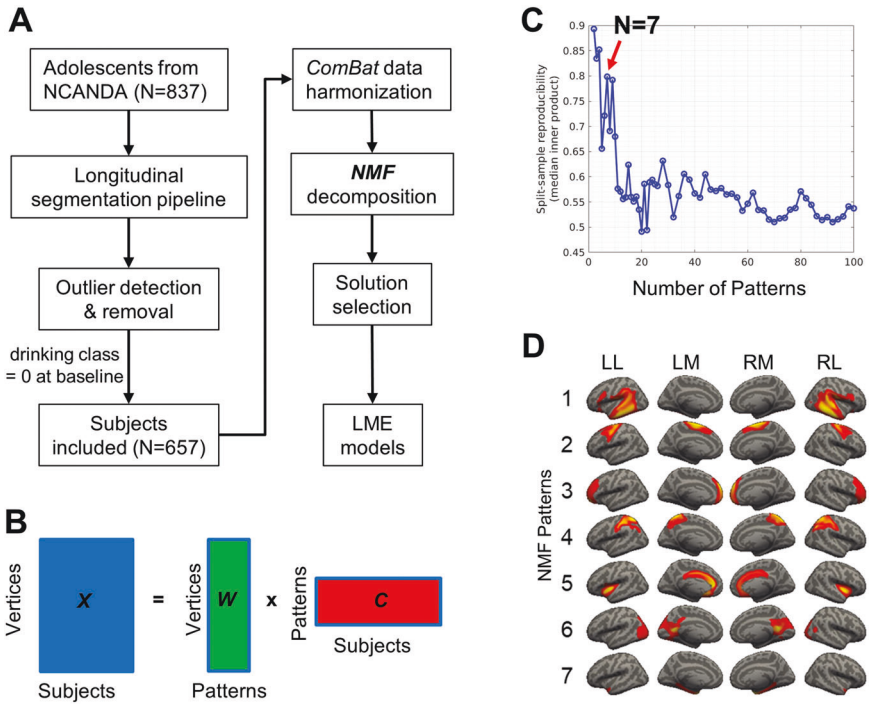

Fig. 1 Analyses pipeline and non-negative matrix factorization (NMF) solutions. A Analyses pipeline. **B** NMF finds the solution that minimizes the difference between the raw data ***X*** and the reconstructed sample represented by the product of ***W*** and ***C***. In matrix ***X***, each row corresponds to a cortical vertex and each column corresponds to a subject. In matrix ***W***, each row corresponds to the cortical thickness of a vertex and each column corresponds to an NMF pattern. In matrix ***C***, each row corresponds to a NMF pattern and each column corresponds to a subject. **C** The optimal number of NMF patterns is 7 based on peaks of the split-sample reproducibility analyses results (NMF solutions ranged from 2 to 100 patterns). **D** The optimal solution of 7 NMF patterns. Pattern 1 contains voxels in angular gyrus, supramarginal gyrus, inferior frontal areas, and superior/middle/inferior temporal regions; pattern 2 is related to superior and middle frontal regions; pattern 3 is associated with frontopolar regions; pattern 4 is associated with postcentral regions and superior parietal lobule; pattern 5 is mainly associated with anterior/middle cingulate cortex and bilateral insula; pattern 6 is associated with posterior cingulate areas, lingual gyrus, cuneus, calcarine sulcus, and primary visual cortex; and pattern 7 is related to parahippocampal gyrus. LL left hemisphere lateral view, LM left hemisphere medial view, RM right hemisphere medial view, RL right hemisphere lateral view.

We addressed these challenges with a data-driven method called non-negative matrix factorization (NMF). Conceptually, NMF may be compared to more widely known methods of principal component analysis (PCA) capable of *feature extraction* and independent component analysis (ICA) capable of *source separation* (see Supplementary Material). More generally, NMF has been successfully used in the fields of astronomy, computer vision, and audio signal processing [16, 17]. NMF is a multivariate algorithm that achieves matrix factorization of an *m* x *n* input matrix (*m*: number of vertices; *n*: number of subjects) into two matrices with non-negative elements. Factorization results in two matrices. The first matrix provides cortical thickness measurements organized into rows and spatially covarying patterns organized into columns. The second matrix specifies spatially covarying patterns organized into rows and subjects organized into columns. Here NMF was applied to identify spatial patterns in cortical thickness variation at the vertex-level that are unconstrained by neuroanatomical borders [18].

We analyzed NCANDA data to assess the effects of adolescent binge drinking and its interactions with multiple risk factors including age, sex, ethnicity, socioeconomic status (SES), family history of alcohol use, and lifetime trauma exposure [19]. The NCANDA study sampled a range of adolescent developmental periods within a relatively short timeframe by adopting an *accelerated longitudinal design* (ALD) [20]. While an important advantage of a longitudinal design is that it measures changes within subjects and within cohorts, making it more powerful than a cross sectional design, it nonetheless cannot establish causation [21]. Thus, it is possible that any brain changes we may detect cannot be linked definitively to alcohol use. Subjects, ages 12–22 years, were recruited at baseline and followed longitudinally at yearly intervals for 5 years. We used NMF to delineate covarying *patterns* of cortical thickness in baseline scans, and applied regression modeling to test alcohol-related departures from normal developmental trajectories for each of the covarying patterns. Consistent with prior evidence, we hypothesized that heavy drinking would be associated with more rapid age-related decline in cortical thickness [6].

METHODS AND MATERIALS

Participants

Adolescents ($n = 837$; 12 - 22 years at baseline) were recruited from five sites: University of California at San Diego ($n = 214$), Duke University ($n = 176$), SRI International ($n = 169$), Oregon Health and Science University ($n = 152$), and University of Pittsburgh ($n = 126$). Exclusionary criteria included serious medical, mental health, or learning disorders [19]. Only youth who did not exceed drinking thresholds for alcohol (drinking class = 0, see below; $n = 657$) at baseline were enrolled (Fig. 1A) [19]. Participants, $n = 657$ were assessed at baseline, 576 returned in 1 year for follow-up-1, 536 for follow-up-2, and 484 for follow-up-3, totaling 2628 study visits. This study was approved by the institutional review board at each site. Adult participants provided written informed consent, and minors provided written assent along with consent from a parent/legal guardian.

Clinical and demographic measures

Drinking class reflects drinking behaviors at baseline and yearly thereafter with the Customary Drinking and Drug Use Record (CDDR) [19] into three drinking classes: (1) no/low drinkers, (2) moderate drinkers, and (3) heavy drinkers. No/low drinkers consumed <1×/month, <2 drinks on average, and <4 drinks maximum. Moderate drinkers consumed from a low

frequency of <1×/month with moderate quantity of 2–3 drinks on average and 4–5 drinks maximum up to moderate frequency of 1×/week and low quantity of 2 drinks on average and <4 drinks maximum. Heavy drinkers consumed from moderate frequency of 2×/month with high quantity of 3–4 drinks on average up to a high frequency of 1×/week or more with moderate quantity of 2–3 drinks or high quantity of >4 drinks [22].

Self-identified ancestry: African-American, White, and Other.

SES was quantified using the highest years of education (range 6–20) of either parent [19] into low SES (6–12 years, $n = 47$) and high SES (13–20 years, $n = 610$).

Family history of alcohol use and dependence (AUD) density (range 0–4) was based on AUD in first- and second-degree relatives using the Family History Assessment Module [23].

Cumulative trauma was quantified as the sum of reported DSM-IV or DSM-5 Criterion-A traumatic events. DSM Criterion-A trauma was assessed separately in the subject and one parent at baseline [22].

MRI acquisition

SRI, Duke, and UCSD used a 3 T General Electric (GE) Discovery MR750 scanner and an 8-channel phased-array, receive-only head coil. Pittsburgh and OHSU used a 3 T Siemens TIM TRIO with a 12-channel phased-array, receive-only head coil. The high-resolution 3D T1-weighted scan was acquired in sagittal orientation. On the GE scanners, the IR-FSPGR (Inversion Recovery-Fast SPoiled Gradient Recalled) sequence was used and, on the Siemens scanners, MPRAGE (Magnetization Prepared Rapid Gradient Echo), with a FOV = 240 mm × 240 mm, acquisition matrix 256 × 256 and slice thickness 1.2 mm. Other parameters for IR-FSPGR were TR/TI/TE = 5.912/400/1.932 ms, flip angle = 11°, 146 slices and, for MPRAGE, TR/TI/TE = 1900/900/2.92 ms, flip angle = 9°, 160 slices.

Analysis overview

Data analysis consisted of 5 major steps. (1) We assembled the relevant imaging, clinical, and demographic data from 5 NCANDA sites for 4 timepoints. (2) We generated vertex-wise cortical surface maps of each participant at each time point using the longitudinal FreeSurfer stream. (3) We performed harmonization of cortical thickness data to account for site and scanner effects using *ComBat*. (4) We applied a multivariate, hypothesis-free method, called non-negative matrix factorization (NMF) to identify image features based on vertex-level patterns of covarying cortical thickness using baseline (first timepoint) scans (5) The mean cortical thickness of 7 covariance patterns from step #4 were used as the dependent variables in regression analyses designed to assess time-related changes in cortical thickness associated with alcohol use. Independent variables included drinking class, cohort age, within person age change, ancestry, SES, family history of alcohol use, lifetime trauma exposure, and participant ID. (5) We used regression analyses to test interactions of drinking class, within-person age change, and cohort age.

Longitudinal segmentation pipeline

FreeSurfer v6.0 longitudinal segmentation was applied using the 4-step longitudinal processing stream [22, 24]. T1 scans for 4 timepoints per subject were supplied to the longitudinal pipeline. The pipeline created an average template from all timepoints. The segmentation of each subject's first timepoint scan used this template as an initial estimate to make the segmentation unbiased by time. The process generated 4 segmentations of the T1 scan, which were processed in the usual manner in native space, and 4 T1 longitudinal segmentations in template space [24]. One participant failed FreeSurfer longitudinal processing.

Outlier detection and removal

Vertices whose cortical thickness were more than 3 standard deviations from the mean of longitudinal scans were removed as outliers. A specific vertex could be excluded, but the remaining vertices for the same subject at other timepoints were retained.

Data harmonization across sites

Harmonization of cortical thickness data from multiple sites/scanners was achieved with *ComBat* that removes scanner/site effects while preserving inherent biological associations such as age, sex, drinking class etc. The tool models expected imaging features as linear combinations of the biological variables and scanner/site effects whose error term is further modulated by site-specific scaling factors [25]. *ComBat* applies empirical Bayes to improve the estimation of site parameters by effectively removing unwanted sources of scanner/site variability while simultaneously increasing the power and reproducibility of subsequent statistical analyses of multi-site cortical thickness studies [25].

NMF

The spatial patterns in cortical thickness were estimated using NMF [18], which weights cortical thickness values that covary within the template to generate highly specific and reproducible pattern-based representations. NMF finds *patterns* of covariance that are common to all participants, such that a combination of these *patterns* with non-negative values approximates the original data. To achieve this, we first organized the cortical thickness data into a non-negative m x n matrix $\boldsymbol{X}$ with m vertices and n participants. We then represented the membership of the vertex-wise cortical thickness values to patterns of structural covariance using an m x v matrix $\boldsymbol{W}$ with m vertices and v patterns. We also represented the contribution of each pattern to the whole cortical thickness map per participant with a v x n matrix $\boldsymbol{C}$ with v patterns and n participants. The NMF algorithm minimized the difference between the raw data $\boldsymbol{X}$ and the reconstructed sample represented by the product of $\boldsymbol{W}$ and $\boldsymbol{C}$ (Fig. 1B). Since matrix decomposition is generally not exactly solvable, we approximate it numerically with NMF. The cortical thickness values in the data matrix $\boldsymbol{X}$ that tend to covary are positively weighted, thus minimizing the reconstruction error and aggregating variance. The non-negativity constraint results in a non-overlapping pattern-based representation of whole-brain cortical thickness, which boasts advantageous specificity [18].

NMF was applied to cortical thickness maps from the baseline scans of 657 no/low drinkers to obtain basis vectors of cortical thickness that capture normal adolescent growth with minimal drinking at baseline. The cortical thickness maps of all participants' longitudinal scans were projected onto the basis vectors to obtain the participant-wise coefficients for each basis vector. All participants have the same number of patterns irrespective of cohort or data source. NMF was run with MATLAB scripts (https://github.com/sundelinustc/NCANDA_NMF).

Solution selection

The NMF algorithm provides many possible solutions to matrix decomposition, each containing a different number of patterns. A solution with too many patterns may overfit the data by modeling noise fluctuations, while too few patterns may combine inherently distinct patterns, which inadequately models the underlying heterogeneity. We determined the optimal number of patterns between 2 and 100 based on reproducibility of data split into two sex- and age-matched halves [18]. We calculated reproducibility across patterns by measuring the overlap between independently estimated patterns from the inner product of the two splits using the Hungarian Algorithm for combinatorial optimization [26].

Study design of NCANDA

NCANDA is a longitudinal study of age-related developmental brain changes associated with adolescent alcohol use that is designed to investigate both within-subject and within-cohort changes. *Within-person age change* represents the difference between the age at each scan and the mean age across visits of a subject. Thus, positive within-person age change corresponds to later visits, whereas negative change corresponds to earlier visits relative to the sample mean. For example, if a participant was scanned at 12, 13, 14, and 15 years old, then the mean of scan age is 13.5 years, and the corresponding within-person age changes are −1.5, −0.5, 0.5, and 1.5 years, respectively. *Cohort-age* represents the difference between a subject's mean age across visits and the mean age of the entire sample across timepoints, thus centering cohort-age at the sample mean. Each participant's cohort-age remained constant across timepoints. For example, if the average age across all participants is 15 years, the above participant's cohort age is 13.5–15 = −1.5 years.

Statistical analyses

We modeled the developmental trajectories of cortical thickness using a linear mixed-effects (LME) approach [20]. In all models, participant identity was included as a random intercept to account for within-subject covariance across time. Drinking class, within-person age change, cohort-age, sex, self-identified ethnicity, SES, family history of AUD density, and cumulative lifetime trauma at baseline visit were included as fixed-effects variables. We investigated the main effect of drinking class; the two-way interactions between drinking class and each of the other fixed-effects

variables; and three-way interactions between drinking class, within-person age change and cohort-age (without two-way interactions), on each of the NMF-derived patterns. The dependent variable for each regression model was the mean cortical thickness at vertices in a given pattern. We also tested the main effects of within-person age change and cohort-age as well as their two-way interaction.

All statistical analyses were conducted in RStudio using *lme4*. The *sjPlot* package was used to plot the significant main and interaction effects. The false discovery rate (FDR) method [27] with a *q-value* threshold of 5% was applied to correct for multiple comparisons corresponding to the number of NMF patterns.

RESULTS

Clinical and behavioral results

See Table 1 for sample demographic and alcohol use characteristics stratified by study visit. See Table 2 for demographic characteristics organized by site at the baseline visit. See Supplementary Table S1 for demographic and clinical characteristics organized by visit and site.

NMF patterns

We identified the optimal number of NMF patterns was 7 based on the most prominent peak in split-sample reproducibility (Fig. 1C). We did not choose 2 or 4 patterns because too few patterns may fail to model the underlying heterogeneity. We also reported the findings for 9 patterns (see SF6) in the Supplementary Materials.

All seven patterns were symmetric bilaterally. As shown in Fig. 1D, Pattern-1 contains the angular gyrus, supramarginal gyrus, inferior frontal gyrus, and superior/middle/inferior temporal cortex. Pattern-2 covers the superior and middle frontal regions. Pattern-3 covers frontopolar cortex. Pattern-4 covers the post-central and superior parietal cortex. Pattern-5 covers the anterior/middle cingulate cortex and bilateral insular cortex. Pattern-6 covers the posterior cingulate gyrus, lingual gyrus, cuneus, calcarine sulcus, and primary visual cortex. Pattern-7 covers the parahippocampal gyrus.

Main effect of cohort-age

Older cohort-age was associated with lower cortical thickness in all 7 patterns (β-values $= -0.826 \sim -0.127$, t-values $= -12.050 \sim -2.574$, q-values < 0.01; Table 3, SF1).

Main effect of within-person age change

Older within-person age was associated with lower cortical thickness in all 7 patterns (β-values $= -1.382 \sim -0.241$, t-values $= -42.812 \sim -12.166$, q-values < 0.001; Table 3, SF2).

Main effect of drinking class

Higher drinking class, indicative of heavier drinking, was associated with lower cortical thickness in pattern-2 (β-value $= -0.215$, t-value $= -2.752$, q-value $= 0.042$; Table 3, SF3) but not the other patterns (β-values $= -0.180 \sim 0.001$, t-values $= -2.014 \sim 0.023$, q-values > 0.1).

Interaction of within-person age change and cohort-age

Significant interaction between within-person age change and cohort-age was found in 6 patterns (β-values $= 0.046 \sim 0.167$, t-values $= 3.757 \sim 13.340$, q-values < 0.001) except for pattern-7 (β-value $= 0.012$, t-value $= 1.534$, q-value $= 0.125$). As shown in Table 4, SF4, older cohorts had a slower rate of within-person age-related cortical thickness decline as compared to younger cohorts.

Interaction of drinking class and cohort-age

Significant interactions were found in 6 patterns (β-values $=$ 0.134–0.249, t-values $=$ 3.887–6.867, q-values < 0.001) except

Table 1. Demographics and clinical characteristics at baseline and follow-ups.

Variable	Baseline ($n = 657$)	Follow-up 1 ($n = 576$)	Follow-up 2 ($n = 536$)	Follow-up 3 ($n = 484$)
Drinking Class				
Low/No	657	482	383	299
Moderate	0	68	93	105
Heavy	0	26	60	80
Sex				
Females	329	288	265	246
Males	328	288	271	238
Age at Scan (Years)				
Mean	15.6	16.8	17.7	18.7
SD	2.3	2.3	2.3	2.3
Self-declared Ancestry				
White	483	428	401	359
African American	92	77	73	63
Other	82	71	62	62
Socioeconomic Status				
6–12 years	47	37	37	36
13–20 years	610	539	499	448
Family History Alcohol Density				
Mean Score	0.20	0.00	0.17	0.16
SD	0.46	0.05	0.40	0.35
Cumulative Traumatic Events				
Mean	1.01	1.01	1.00	1.00
SD	1.04	1.05	1.03	1.05

Note: Socioeconomic status (SES) was quantified using the highest years of education of either parent.

Table 2. Demographic Characteristics at Baseline by Site.

	Pittsburgh ($n = 92$)	SRI ($n = 126$)	Duke ($n = 140$)	OHSU ($n = 130$)	UCSD ($n = 169$)
Sex					
Females	50	59	73	65	82
Males	42	67	67	65	87
Age at Scan (Years)					
Mean	16.2	15.0	15.2	16.1	15.8
SD	2.5	1.9	1.9	2.6	2.4
Self-declared ancestry					
White	71	98	76	109	129
African American	19	1	55	3	14
Other	2	27	9	18	26
Socioeconomic Status					
6-12 years	7	4	12	7	17
13-20 years	85	122	128	123	152
Family History Alcohol Use Density					
Mean Score	0.12	0.24	0.09	0.22	0.31
SD	0.30	0.60	0.24	0.43	0.54
Cumulative Traumatic Events*					
Mean	0.87	0.52	1.41	1.20	0.99
SD	1.13	0.80	0.94	1.21	0.98

Socioeconomic status (SES) was quantified using the highest years of education of either parent.
Pittsburg University of Pittsburgh Medical Center, *SRI* SRI International, *Duke* Duke University Medical Center, *OHSU* Oregon Health and Science University, *UCSD* University of California at San Diego.
*No participant met DSM criteria for PTSD at baseline.

pattern-7 (β-value = 0.031, t-value = 1.386, q-value = 0.166). As shown in Table 4, SF5, higher drinking class was associated with a slower rate of cohort-age-related cortical thickness decline.

Interaction of drinking class and within-person age change

No significant result was found in any pattern (β-values = −0.073–0.162, t-values = −1.592–2.480, q-values > 0.09; Table 4).

Interaction of drinking class, cohort-age and within-person age change

Significant three-way interactions were found in all patterns (β-values = 0.065–0.182, t-values = 2.842–8.002, q-values < 0.01) except for pattern-7 (β-value = 0.011, t-value = 0.725, q-value = 0.469). As shown in Table 4 and Fig. 2, the longitudinal rate of cortical thickness decline in no/low drinkers was similar for all age cohorts. The decline among moderate drinkers was faster in the younger cohort and slower in the older cohort. The decline among heavy drinkers was fastest in the younger cohort and slowest in the older cohort.

Interaction of drinking class and other variables

There were no significant interactions between drinking class and the other variables including sex, cumulative trauma, self-identified ethnicity, SES, family history of AUD (see Supplementary Table S2).

DISCUSSION

We investigated the longitudinal link between heavy drinking behavior and cortical development in a large adolescent sample. We applied NMF, a multivariate data-driven method, to cluster vertices into 7 covarying patterns of cortical thickness. Significant decline in cortical thickness was modulated by cohort-age (Supplementary Fig. S1) and longitudinal progression (within-person age change; Supplementary Fig. S2) in all 7 patterns. Participants in older cohorts, relative to younger cohorts, experienced slower declines in cortical thickness associated with drinking across longitudinal visits for 6 patterns (Supplementary Fig. S4). Adolescents who engaged in heavy drinking experienced slower cohort-age associated declines in cortical thickness across 6 patterns (Supplementary Fig. S5) and exhibited lower cortical thickness in pattern 2 (superior and middle frontal regions; Supplementary Fig. S3). Of particular interest, the longitudinal rate of cortical thickness decline was similar for all age cohorts among no/low drinkers in widely distributed regions (6 patterns) over longitudinal study visits. However, moderate and heavy drinking was differentially linked to the trajectory of cortical thinning across age cohorts. Specifically, cortical thinning among moderate drinkers was faster in the younger cohort and slower in the older cohort, whereas cortical thinning among heavy drinkers was fastest in the younger cohort and slowest in the older cohort (Fig. 2).

Our results confirm that cortical thinning, a process typical of adolescent brain development, is particularly pronounced among younger adolescents engaged in heavy drinking, and considerably attenuated with heavy drinking in older adolescents [14]. The present study is the largest to investigate cortical gray matter changes associated with adolescent alcohol use and the first to deploy unsupervised machine learning capable of identifying coordinated patterns of cortical thickness variation that are unconstrained by neuroanatomical boundaries [18]. A small number of strongly affected patterns are expected to be more sensitive at capturing statistically significant results than region-of-interest methods, which lack spatial localization to affected areas, and whole brain vertex-wise analysis [14], which must survive stringent corrections for multiple comparisons. Consequently, both methods suffer from Type II error. Interestingly, the patterns identified by NMF are closely related to meaningful functional networks that recapitulate established patterns in large normative adolescent samples [18].

Table 3. Main effects of drinking class, within-person age change, and cohort-age per NMF pattern.

Pattern	β	SD	df	t	p	q	Adj. R^2
Main effect of drinking class							
1	−0.152	0.081	1699.0	−1.873	0.061	0.143	0.909
2	−0.215	0.078	1696.3	−2.752	0.006	0.042	0.895
3	−0.110	0.092	1715.3	−1.194	0.233	0.326	0.897
4	−0.180	0.090	1713.1	−2.014	0.044	0.143	0.890
5	0.032	0.062	1711.0	0.520	0.603	0.704	0.898
6	−0.086	0.070	1705.9	−1.221	0.222	0.326	0.901
7	0.001	0.050	1670.6	0.023	0.982	0.982	0.916
Main effect of within-person age change							
1	−1.382	0.032	1617.0	−42.812	<0.001	<0.001	0.909
2	−0.766	0.031	1615.5	−24.647	<0.001	<0.001	0.895
3	−1.373	0.037	1620.6	−37.328	<0.001	<0.001	0.897
4	−1.096	0.036	1618.4	−30.649	<0.001	<0.001	0.890
5	−0.956	0.025	1617.8	−38.644	<0.001	<0.001	0.898
6	−0.963	0.028	1616.1	−34.401	<0.001	<0.001	0.901
7	−0.241	0.020	1611.1	−12.166	<0.001	<0.001	0.916
Main effect of cohort-age							
1	−0.702	0.069	658.5	−10.219	<0.001	<0.001	0.909
2	−0.396	0.067	657.2	−5.933	<0.001	<0.001	0.895
3	−0.826	0.073	659.7	−11.342	<0.001	<0.001	0.897
4	−0.672	0.071	657.4	−9.468	<0.001	<0.001	0.890
5	−0.596	0.049	657.1	−12.050	<0.001	<0.001	0.898
6	−0.638	0.057	656.0	−11.177	<0.001	<0.001	0.901
7	−0.127	0.049	656.9	−2.574	0.010	0.010	0.916

Note: the regression model is "y ~ cohort-age + within-person age change + drinking class + sex + ethnicity + SES + family history of AUD density + life trauma + (1|participant ID)". y is the mean cortical thickness of a pattern. β, fixed-effect regression coefficient; *SD* standard deviation, *df* degree of freedom; *t*, *t* value; *p*, uncorrected *p*-value; q, FDR corrected *p*-value; Adj. R2, adjusted R^2.

Pattern-1 (Fig. 1D) is aligned with the language network, which has dorsal and ventral pathways. The dorsal pathway connects the temporal cortex and premotor cortex to effect speech to posterior Broca's area to effect syntactic processes while ventral pathways effect semantic process [28]. Motor and premotor regions are relevant for language production, while auditory and visual systems are recruited for language perception. Adult AUD is implicated in both structural and functional alterations of the language network [29, 30], while heavy drinking in adolescents is implicated in gray matter decline of the language network that involves middle temporal, superior temporal cortex and temporoparietal cortex [6, 31]. Pattern-6 is aligned with the visual network, which plays a vital role in perception. Rodent models reveal ethanol disrupts the critical period of visual cortical development, which includes the adolescence [32]. Human adolescents engaging in heavy use similarly manifest lower functional activity in the visual network including the occipital lobe and cuneus [33]. Pattern-2 aligns with the sensorimotor network including motor and premotor regions that are impacted negatively by adolescent alcohol use [29]. Pattern-4 coincides with the dorsal attention network (DAN) that exhibits increased activity during the voluntary orienting of attention by the frontal eye fields, the intraparietal sulcus (IPS), and superior parietal lobe (SPL). Reduced white matter connectivity of the DAN is reflected as behavioral deficits of impulsivity, inattention, and risk taking [34]. Notably, increased connectivity in the DAN is linked to adolescent alcohol use, adolescent ADHD, and is most increased in comorbid adolescent alcohol use and ADHD [35]. Relatedly alcohol use disorder is 5-fold higher in ADHD than individuals without ADHD.

Adolescent binge drinking is linked to impaired executive function, which is consistent with findings that link adolescent binge drinking to weaker frontoparietal connectivity [36] and reduced prefrontal activation [37–39]. Pattern-5 includes the anterior and middle cingulate cortices and bilateral insula that encompass the salience network (SN). The SN plays a crucial role in consciously integrating autonomic feedback and responses with internal goals and external demands [40], and in response inhibition [41]. Adolescents who engage in binge drinking require increased effort when inhibiting prepotent responses to alcohol-related stimuli by engaging bilateral anterior insula and inferior frontal gyrus, both of which are core components of the SN [42], and depend on intact FPN function. The posterior cingulate cortex and precuneus within pattern-6 and the anterior cingulate cortex within pattern-5 are key components of the default mode network (DMN). Self-referential processing, theory of mind (ToM), memory, and learning [43], which are active in the absence of goal-directed activity, are characteristic functions of the DMN. Notably, the DMN is dysregulated in adolescents with family history of AUD [44] and adolescent binge drinkers have heightened connectivity between DMN regions, which impedes the maturation of affective and self-reflective neural systems [45], and undermines the development of complex social and emotional behaviors that are important in transition to adulthood [46]. Thus, our findings in language, visual, sensorimotor, and dorsal attention networks, which are integral to adolescent brain development [47], are consistent with evidence that adolescent alcohol exposure alters network activity and reconfigures network connectivity [48]. Our NMF-derived findings may help to guide future hypothesis-driven investigations of alcohol effects on adolescent brain development.

Table 4. Interaction effects among drinking class, within-person age change, and cohort-age per NMF-derived pattern.

Pattern	β	SD	df	t	p	q	Adj. R^2
Drinking class x within-person age change interaction[1]							
1	0.031	0.075	1615.1	0.416	0.678	0.790	0.909
2	−0.033	0.073	1613.5	−0.458	0.647	0.790	0.895
3	0.126	0.086	1618.6	1.475	0.140	0.327	0.897
4	0.096	0.083	1616.5	1.156	0.248	0.433	0.890
5	−0.002	0.058	1615.8	−0.033	0.973	0.973	0.898
6	0.162	0.065	1614.1	2.480	0.013	0.093	0.901
7	−0.073	0.046	1609.2	−1.592	0.112	0.327	0.916
Drinking class x cohort-age interaction[2]							
1	0.237	0.036	1687.5	6.629	<0.001	<0.001	0.912
2	0.135	0.035	1686.5	3.887	<0.001	<0.001	0.896
3	0.238	0.041	1702.9	5.817	<0.001	<0.001	0.899
4	0.249	0.040	1700.3	6.271	<0.001	<0.001	0.893
5	0.134	0.028	1699.3	4.847	<0.001	<0.001	0.899
6	0.213	0.031	1693.4	6.867	<0.001	<0.001	0.903
7	0.031	0.022	1663.6	1.386	0.166	0.166	0.916
Within-person age change x cohort-age interaction[3]							
1	0.161	0.012	1597.5	13.339	<0.001	<0.001	0.919
2	0.046	0.012	1596.8	3.757	<0.001	<0.001	0.896
3	0.167	0.014	1598.5	11.990	<0.001	<0.001	0.906
4	0.153	0.014	1596.5	11.233	<0.001	<0.001	0.898
5	0.106	0.009	1596.1	11.227	<0.001	<0.001	0.905
6	0.140	0.011	1595.1	13.340	<0.001	<0.001	0.910
7	0.012	0.008	1597.0	1.534	0.125	0.125	0.916
Drinking class x within-person age change x cohort-age interaction[4]							
1	0.161	0.024	1621.7	6.810	<0.001	<0.001	0.912
2	0.065	0.023	1620.7	2.842	<0.001	<0.001	0.895
3	0.182	0.027	1626.5	6.786	<0.001	<0.001	0.900
4	0.166	0.026	1624.4	6.347	<0.001	<0.001	0.893
5	0.094	0.018	1623.9	5.152	<0.001	<0.001	0.899
6	0.163	0.020	1621.1	8.002	<0.001	<0.001	0.904
7	0.011	0.015	1614.6	0.725	0.469	0.469	0.915

Note: regression models are
1. y ~ cohort-age + within-person age change * drinking class + sex + ethnicity + SES + family history of AUD density + life trauma + (1|participant ID);
2. y ~ within-person age change + cohort-age * drinking class + sex + ethnicity + SES + family history of AUD density + life trauma + (1|participant ID);
3. y ~ within-person age change * cohort-age + drinking class + sex + ethnicity + SES + family history of AUD density + life trauma + (1|participant ID);
4. y ~ within-person age change: cohort-age: drinking class + sex + ethnicity + SES + family history of AUD density + life trauma + (1|participant ID).
y is the mean cortical thickness of a pattern. β, fixed-effect regression coefficient; *SD* standard deviation, *df* degree of freedom; *t*, *t* value; *p*, uncorrected *p* value; q, FDR corrected *p* value. Adj. R2, adjusted R^2.

The typical pattern of (within-person) age-related cortical thinning, which is more rapid in younger cohorts than older cohorts in moderate drinkers, is still more rapid in heavy drinkers. (Table 4, Fig. 2). Greater frequency and intensity of alcohol use in older cohorts coincided with powerful neurotoxic effects during early study visits and/or more profound delays in brain maturation via pruning during late visits [30]. By contrast, alcohol consumption in younger cohorts coincided with delayed cortical maturation during early visits and/or severe neurotoxic effects during late visits. Relatedly, Squeglia et al. [6] reported faster grey matter reduction only in adolescents engaged in heavy drinking. Studies using anatomically defined ROIs obscured the underlying heterogeneity in age-related cortical thinning associated with synaptic pruning, but were revealed by unsupervised machine learning. Indeed, cortical areas that undergo marked pruning during adolescence are particularly susceptible to the effects of heavy alcohol consumption [49].

Through rapid remodeling of the brain, frontal- and parietal-lobe gray matter reaches maximum size at 12 years in males and 10.2–11 years in females. The maximum size of other brain regions, such as the temporal-lobe gray matter, is achieved at 16.5 years for males and 16.7 females. While new synaptic connections are made, others are pruned, a process shaped by experience and environment, to make the adolescent brain extraordinarily versatile. In this context, while research in humans has established cognitive, behavioral, and gross volume effects of alcohol on the adolescent brain, only animal models have mapped the cellular, synaptic, and molecular mechanisms underlying this maturation. Although direct evidence of neurotoxicity in adolescents is lacking in humans, the neurotoxic effects of alcohol on the adolescent rat brain are found in frontal anterior, olfactory, and anterior perirhinal cortices. Intermittent alcohol intake in rats produces neuroinflammation, disrupted neurogenesis, and epigenetic

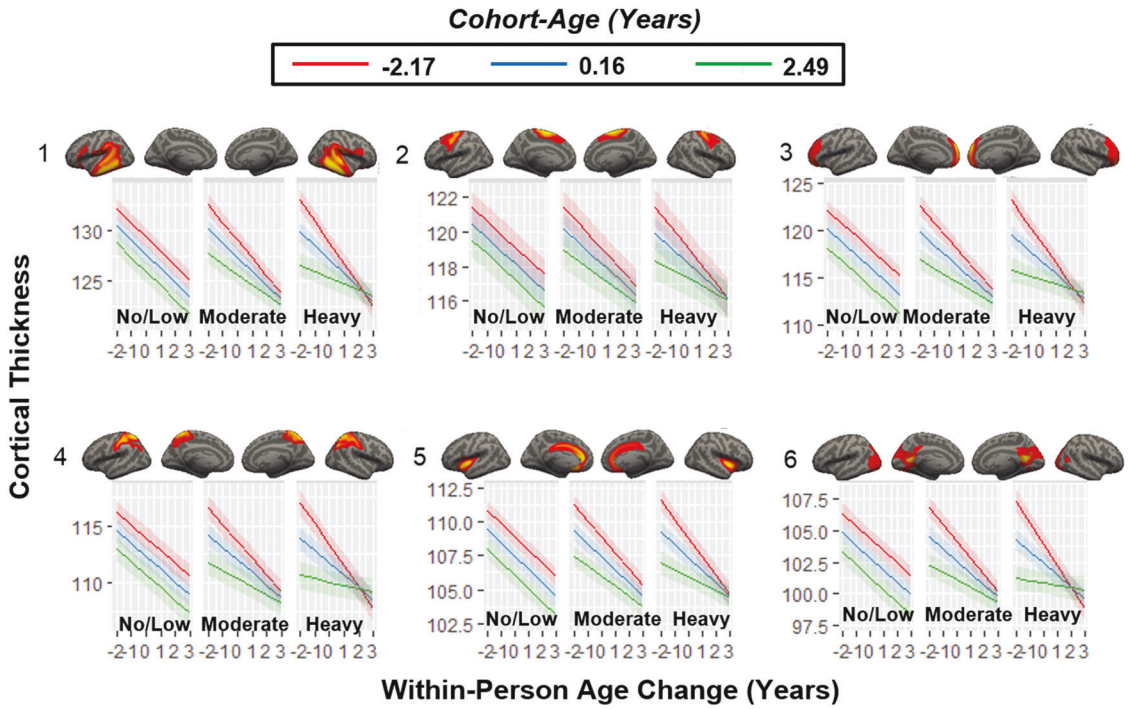

Fig. 2 Three-way interactions between drinking class, cohort-age and within-person age change. The rates of within-person age-related cortical thickness declines are similar across age cohorts in no/low drinkers, faster in the younger cohort and slower in the older cohort in moderate drinkers, and fastest in the younger cohort and slowest in the older cohort in heavy drinkers for all patterns (β-values = 0.065–0.182, t-values = 2.842–8.002, q-values < 0.01) except for pattern 7 (β-value = 0.011, t-value = 0.724, q-value = 0.469). The x-axis represents the within-person age change in years.

modifications, leading to neural death in the prefrontal cortex with lasting behavioral consequences [50]. Indeed, some adolescent neural disruptions persist into adulthood [30].

The NCANDA longitudinal design enabled us to investigate age-related developmental changes during adolescence coupled with the effects of alcohol use. Furthermore, the ALD permits more rapid enrollment (larger pool of potential participants), faster study completion (wider age range at baseline and each timepoint), and suffers from less study dropout (shorter study duration), than a single cohort design. The advantages of ALD are accrued because all available individuals in the specified age-range are accepted. By contrast, the single cohort longitudinal design requires all participants are the same age. Random and fixed cohort effects in our regression modeling addressed possible bias introduced by multiple cohorts. However, inherent missing data is a limitation of the design where each subject's measurement schedule covers only a part of the age-range of interest. This may limit inferences if an age-cohort effect is present that leads to systematic differences between subjects born at different times.

Our analysis of longitudinal vertex-wise data posed several challenges in the context of NMF. The straightforward application of NMF to 2D data (vertices, subjects) from a cross sectional study posed challenges for the analysis of 3D data (vertices, subjects, timepoints) from a longitudinal study. Namely, the factorization of 3D matrices is problematic because 3D space is a continuum, which means the non-negative representation of 3D coordinates is non-trivial [51]. An alternative approach was to reduce dimensionality at each vertex by using the slope of the line fitted to the longitudinal cortical thickness measurements. However, this presented challenges to interpreting negative vs positive slopes, and noise associated with a line fitted to only 4 data points. Thus, we elected to use 2D matrix factorization to identify cortical thickness patterns only at the baseline visit. Then the longitudinal change in cortical thickness of these vertex patterns was assessed in relation to age, alcohol use, and other regressors. A potential limitation of our approach is that age of alcohol use may impact regions outside the vertices contained in the 7 patterns that we interrogated. Furthermore, our results for the regressors sex, cumulative trauma, self-identified ethnicity, SES, and family history of AUD were negative within the 7 patterns, it is possible these regressors may be significantly associated with vertices outside these 7 patterns. Other NCANDA studies found that baseline PTSD symptoms, predicted a longitudinal course of moderate to heavy drinking [52] and cumulative lifetime trauma and adolescent alcohol use interact to affect the volume and trajectory of hippocampal and amygdala subregions [22]. It is possible that specific variables in adolescent drinkers, such as sex and trauma have stronger effects on cortical volume, surface area, and subcortical volume [22] than on cortical thickness. Studies reported thicker cortices in adolescent female binge drinkers ($n = 14$) than female controls ($n = 15$), while thinner cortices in adolescent male binge drinkers ($n = 15$) than male controls ($n = 15$) in frontal pole, pars orbitalis, medial orbital frontal, and rostral anterior cingulate areas [13], and thinner medial and lateral rostro-frontal and superior parietal cortices in adolescents with a family history of AUD ($n = 93$) than controls ($n = 95$), especially among the youngest adolescents [53]. Interactions between alcohol consumption and sex [13], or family history of AUD [53] in relatively small samples with specific clinical and demographic attributes may not generalize to our much larger and more representative sample. Large-scale studies of adolescent cortical development that assess the role of alcohol with other environmental insults such as childhood trauma, poverty, drug use, neighborhood deprivation, and education may prove to be informative.

Strengths and limitations

The first limitation is that no global minimum of the cost function is guaranteed with NMF because only local minima are provided [54]. Consequently, several NMF runs are necessary to avoid

getting stuck in a local minimum. Second, although cannabis use occurred at extremely low levels in our sample, it is associated with accelerated cortical thinning, but we did not control for cannabis use [55]. Third, we analyzed the first four years of NCANDA data, but another time point became available as we concluded data analyses. Adding this data will temporally expand the observation of each developmental cohort and may help define longer-term sequelae. Fourth, the association of brain changes with specific cognitive or behavioral impairments that accompany adolescent alcohol use were not investigated. Fifth, while we did not correlate the NMF patterns with cognitive and behavioral measurements directly, the behavioral and cognitive impairments associated with drinking in this sample are well documented. A detailed account is available in Sullivan et al. [56]. Briefly, the heavy drinking group from NCANDA performed significantly below the no/low-drinking group on balance accuracy (postural stability), general ability (vocabulary, math calculation, word reading), attention, episodic memory, emotion (recognition), faster motor speed at the expense of diminished accuracy, and delay discounting performance, which showed poor impulse control in the heavy drinkers regardless of age. Finally, our analysis was limited to cortical thickness data, but did not examine cortical surface area or white matter. Future studies that apply multi-modal imaging may discover novel effects of alcohol in the adolescent brain to inform treatment development.

Our study has several strengths relative to previous investigations. First, we applied unsupervised machine learning to achieve clustering, feature extraction, source separation, and data dimension reduction, all of which enhanced statistical power. Second, we investigated three times more participants than any previous study. Third, we utilized *ComBat* to harmonize cortical thickness measurements across five NCANDA sites to preserve variance associated with neurobiologically and behaviorally relevant variables [25, 57]. Finally, we leveraged longitudinal data with four yearly timepoints, which is extraordinarily rare among neuroimaging studies of psychiatric conditions.

CONCLUSIONS

Unsupervised machine learning capable of *feature extraction* and *source selection* can identify spatial patterns of vertex-level cortical thickness variation. Age-related cortical thinning, which is typical of the adolescent neurodevelopment process, occurs more rapidly in younger individuals and less rapidly in older individuals who engage in heavy alcohol consumption as compared to low/non-drinking adolescents. Early adolescent binge drinking is negatively associated with profoundly consequential processes of neuromaturation. Future studies are certain to elucidate their effects on wide-ranging processes of cognitive, emotional, and social learning.

DATA AVAILABILITY

Data used here are from the data release NCANDA_PUBLIC_3Y_REDCAP_V03 (https://doi.org/10.7303/syn23702728) and NCANDA_PUBLIC_3Y_STRUCTURAL_V01 (https://doi.org/10.7303/syn22213272) distributed to the public according to the NCANDA Data Distribution agreement (www.niaaa.nih.gov/research/major-initiatives/nationalconsortium-alcohol-and-neurodevelopment-adolescence/ncandadata).

REFERENCES

1. Tamnes CK, Herting MM, Goddings AL, Meuwese R, Blakemore SJ, Dahl RE, et al. Development of the cerebral cortex across adolescence: a multisample study of inter-related longitudinal changes in cortical volume, surface area, and thickness. J Neurosci. 2017;37:3402–12.
2. Pfefferbaum A, Rohlfing T, Pohl KM, Lane B, Chu WW, Kwon D, et al. Adolescent development of cortical and white matter structure in the NCANDA sample: role of sex, ethnicity, puberty, and alcohol drinking. Cereb Cortex. 2016;26:4101–21.
3. Amlien IK, Fjell AM, Tamnes CK, Grydeland H, Krogsrud SK, Chaplin TA, et al. Organizing principles of human cortical development-thickness and area from 4 to 30 years: insights from comparative primate neuroanatomy. Cereb Cortex. 2016;26:257–67.
4. Lees B, Meredith LR, Kirkland AE, Bryant BE, Squeglia LM. Effect of alcohol use on the adolescent brain and behavior. Pharmacol Biochem Behav. 2020;192:172906.
5. Cservenka A, Brumback T. The burden of Binge and heavy drinking on the brain: effects on adolescent and young adult neural structure and function. Front Psychol. 2017;8:1111.
6. Squeglia LM, Tapert SF, Sullivan EV, Jacobus J, Meloy MJ, Rohlfing T, et al. Brain development in heavy-drinking adolescents. Am J Psychiat. 2015;172:531–42.
7. Johnston LD, Miech RA, O'Malley PM, Bachman JG, Schulenberg JE, Patrick ME. "Monitoring the Future National Survey Results on Drug Use, 1975-2018: Overview, Key Findings on Adolescent Drug Use." Institute for Social Research (2019).
8. Chung T, Creswell KG, Bachrach R, Clark DB, Martin CS. Adolescent Binge drinking developmental context and opportunities for prevention. Alcohol Res-Curr Rev. 2018;39:5–15.
9. SAMHSA. U.S. Department of Health and Human Services (HHS), Substance Abuse and Mental Health Services Administration (SAMHSA), 2018.
10. Wilson S, Malone SM, Thomas KM, Iacono WG. Adolescent drinking and brain morphometry: a co-twin control analysis. Dev Cogn Neuros-Neth. 2015;16:130–38.
11. Mashhoon Y, Czerkawski C, Crowley DJ, Cohen-Gilbert JE, Sneider JT, Silveri MM. Binge alcohol consumption in emerging adults: anterior cingulate cortical "thinness" is associated with alcohol use patterns. Alcohol Clin Exp Res. 2014;38:1955–64.
12. Luciana M, Collins PF, Muetzel RL, Lim KO. Effects of alcohol use initiation on brain structure in typically developing adolescents. Am J Drug Alcohol Abus. 2013;39:345–55.
13. Squeglia LM, Sorg SF, Schweinsburg AD, Wetherill RR, Pulido C, Tapert SF. Binge drinking differentially affects adolescent male and female brain morphometry. Psychopharmacol (Berl). 2012;220:529–39.
14. Infante MA, Eberson SC, Zhang Y, Brumback T, Brown SA, Colrain IM, et al. Adolescent Binge drinking is associated with accelerated decline of Gray Matter Volume. Cereb Cortex. 2022;32:2611–20.
15. Jacobus J, Castro N, Squeglia LM, Meloy MJ, Brumback T, Huestis MA, et al. Adolescent cortical thickness pre- and post marijuana and alcohol initiation. Neurotoxicol Teratol. 2016;57:20–9.
16. Lee DD, Seung HS. Learning the parts of objects by non-negative matrix factorization. Nature. 1999;401:788–91.
17. Mirzal A. NMF versus ICA for blind source separation. Adv Data Anal Cl. 2017;11:25–48.
18. Sotiras A, Toledo JB, Gur RE, Gur RC, Satterthwaite TD, Davatzikos C. Patterns of coordinated cortical remodeling during adolescence and their associations with functional specialization and evolutionary expansion. P Natl Acad Sci USA. 2017;114:3527–32.
19. Brown SA, Brumback TY, Tomlinson K, Cummins K, Thompson WK, Nagel BJ, et al. The national consortium on alcohol and neuro-development in adolescence (NCANDA): a multisite study of adolescent development and substance use. J Stud Alcohol Drugs. 2015;76:895–908.
20. Galbraith S, Bowden J, Mander A. Accelerated longitudinal designs: an overview of modelling, power, costs and handling missing data. Stat Methods Med Res. 2017;26:374–98.
21. Wilson S. Commentary: substance use and the brain: it is not straightforward to differentiate cause from consequence - a commentary on Kim-Spoon et al. (2020). J Child Psychol Psychiatry. 2021;62:437–40.
22. Phillips RD, De Bellis MD, Brumback T, Clausen AN, Clarke-Rubright EK, Haswell CC, et al. Volumetric trajectories of hippocampal subfields and amygdala nuclei influenced by adolescent alcohol use and lifetime trauma. Transl Psychiatry. 2021;11:1–13.
23. Bucholz KK, Cadoret R, Cloninger CR, Dinwiddie SH, Hesselbrock VM, Nurnberger JI Jr., et al. A new, semi-structured psychiatric interview for use in genetic linkage studies: a report on the reliability of the SSAGA. J Stud Alcohol. 1994;55:149–58.
24. Reuter M, Schmansky NJ, Rosas HD, Fischl B. Within-subject template estimation for unbiased longitudinal image analysis. Neuroimage. 2012;61:1402–18.
25. Fortin JP, Cullen N, Sheline YI, Taylor WD, Aselcioglu I, Cook PA, et al. Harmonization of cortical thickness measurements across scanners and sites. Neuroimage. 2018;167:104–20.
26. Kuhn HW. The Hungarian Method for the assignment problem. Nav Res Log. 2005;52:7–21.
27. Benjamini Y, Hochberg Y. Controlling the false discovery rate - a practical and powerful approach to multiple testing. J R Stat Soc B. 1995;57:289–300.
28. Friederici AD, Gierhan SM. The language network. Curr Opin Neurobiol. 2013;23:250–4.

29. Fede SJ, Grodin EN, Dean SF, Diazgranados N, Momenan R. Resting state connectivity best predicts alcohol use severity in moderate to heavy alcohol users. Neuroimage Clin. 2019;22:101782.
30. Spear LP. Effects of adolescent alcohol consumption on the brain and behaviour. Nat Rev Neurosci. 2018;19:197–214.
31. Squeglia LM, Rinker DA, Bartsch H, Castro N, Chung Y, Dale AM, et al. Brain volume reductions in adolescent heavy drinkers. Dev Cogn Neurosci. 2014;9:117–25.
32. Crews F, He J, Hodge C. Adolescent cortical development: a critical period of vulnerability for addiction. Pharm Biochem Behav. 2007;86:189–99.
33. Ewing SW, Sakhardande A, Blakemore SJ. The effect of alcohol consumption on the adolescent brain: A systematic review of MRI and fMRI studies of alcohol-using youth. Neuroimage Clin. 2014;5:420–37.
34. Sanefuji M, Craig M, Parlatini V, Mehta MA, Murphy DG, Catani M, et al. Double-dissociation between the mechanism leading to impulsivity and inattention in attention deficit hyperactivity disorder: a resting-state functional connectivity study. Cortex. 2017;86:290–302.
35. Farre-Colomes A, Gerhardt S, Luderer M, Sobanski E, Kiefer F, Vollstadt-Klein S. Common and distinct neural connectivity in attention-deficit/hyperactivity disorder and alcohol use disorder studied using resting-state functional magnetic resonance imaging. Alcohol Clin Exp Res. 2021;45:948–60.
36. Weiland BJ, Sabbineni A, Calhoun VD, Welsh RC, Bryan AD, Jung RE, et al. Reduced left executive control network functional connectivity is associated with alcohol use disorders. Alcohol Clin Exp Res. 2014;38:2445–53.
37. Squeglia LM, Schweinsburg AD, Pulido C, Tapert SF. Adolescent Binge drinking linked to abnormal spatial working memory brain activation: differential gender effects. Alcohol Clin Exp Res. 2011;35:1831–41.
38. Crego A, Rodriguez-Holguin S, Parada M, Mota N, Corral M, Cadaveira F. Reduced anterior prefrontal cortex activation in young binge drinkers during a visual working memory task. Drug Alcohol Depen. 2010;109:45–56.
39. Parada M, Corral M, Mota N, Crego A, Rodriguez Holguin S, Cadaveira F. Executive functioning and alcohol binge drinking in university students. Addict Behav. 2012;37:167–72.
40. Seeley WW. The Salience network: a neural system for perceiving and responding to homeostatic demands. J Neurosci. 2019;39:9878–82.
41. Whelan R, Watts R, Orr CA, Althoff RR, Artiges E, Banaschewski T, et al. Neuropsychosocial profiles of current and future adolescent alcohol misusers. Nature. 2014;512:185.
42. Ames SL, Wong SW, Bechara A, Cappelli C, Dust M, Grenard JL, et al. Neural correlates of a Go/NoGo task with alcohol stimuli in light and heavy young drinkers. Behav Brain Res. 2014;274:382–89.
43. Raichle ME. The Brain's default mode network. Annu Rev Neurosci. 2015;38:433–47.
44. Wetherill RR, Bava S, Thompson WK, Boucquey V, Pulido C, Yang TT, et al. Frontoparietal connectivity in substance-naive youth with and without a family history of alcoholism. Brain Res. 2012;1432:66–73.
45. Muller-Oehring EM, Kwon D, Nagel BJ, Sullivan EV, Chu WW, Rohlfing T, et al. Influences of age, sex, and moderate alcohol drinking on the intrinsic functional architecture of adolescent brains. Cereb Cortex. 2018;28:1049–63.
46. Zeigler DW, Wang CC, Yoast RA, Dickinson BD, McCaffree MA, Robinowitz CB, et al. The neurocognitive effects of alcohol on adolescents and college students. Prev Med. 2005;40:23–32.
47. Baum GL, Cui ZX, Roalf DR, Ciric R, Betzel RF, Larsen B, et al. Development of structure-function coupling in human brain networks during youth. P Natl Acad Sci USA. 2020;117:771–78.
48. Zhao Q, Sullivan EV, Műller-Oehring EM, Honnorat N, Adeli E, Podhajsky S, et al. Adolescent alcohol use disrupts functional neurodevelopment in sensation seeking girls. Addict Biol. 2021;26:e12914.
49. Jones SA, Lueras JM, Nagel BJ. Effects of Binge drinking on the developing brain. Alcohol Res. 2018;39:87–96.
50. Guerri C, Pascual M. Mechanisms involved in the neurotoxic, cognitive, and neurobehavioral effects of alcohol consumption during adolescence. Alcohol. 2010;44:15–26.
51. Koppen WP, Christmas WJ, Crouch DJM, Bodmer WF, Kittler JV. Extending non-negative matrix factorisation to 3D registered data. In 2016 International Conference on Biometrics (ICB), IEEE; 2016. pp. 1–8.
52. De Bellis MD, Nooner KB, Brumback T, Clark DB, Tapert SF, Brown SA. Posttraumatic stress symptoms predict transition to future adolescent and young adult moderate to heavy drinking in the NCANDA sample. Curr Addict Rep. 2020;7:99–107.
53. Henderson KE, Vaidya JG, Kramer JR, Kuperman S, Langbehn DR, O'Leary DS. Cortical thickness in adolescents with a family History of alcohol use disorder. Alcohol Clin Exp Res. 2018;42:89–99.
54. Esposito F. A review on initialization methods for nonnegative matrix factorization: towards omics data experiments. Mathematics. 2021;9:1006.
55. Albaugh MD, Ottino-Gonzalez J, Sidwell A, Lepage C, Juliano A, Owens MM, et al. Association of cannabis use during adolescence with neurodevelopment. JAMA Psychiatry. 2021;78:1031–40.
56. Sullivan EV, Brumback T, Tapert SF, Fama R, Prouty D, Brown SA, et al. Cognitive, emotion control, and motor performance of adolescents in the NCANDA study: contributions from alcohol consumption, age, sex, ethnicity, and family history of addiction. Neuropsychology. 2016;30:449–73.
57. Sun D, Rakesh G, Haswell CC, Logue M, Baird CL, O'Leary EN, et al. A comparison of methods to harmonize cortical thickness measurements across scanners and sites. NeuroImage. 2022;261:119509.

ACKNOWLEDGEMENTS

We would like to recognize Mary Nicole Buckley and Molly Monsour for their help with the visual inspection of segmentations. We also thank the anonymous reviewers for their thoughtful comments and suggestions.

AUTHOR CONTRIBUTIONS

DS analyzed data and drafted the manuscript. VA analyzed data and drafted the manuscript, RP analyzed data. HB drafted the manuscript. AS developed the analysis methods. AM coordinated the research. FB coordinated the research. ST coordinated the research. SB coordinated the research. DC coordinated the research. DG coordinated the research. KN coordinated the research. BN coordinated the research. WT coordinated the research. MDB coordinated and designed the research. RM designed and coordinated the research and drafted the manuscript.

FUNDING INFORMATION

RAM was supported by the Department of Veterans Affairs Mid-Atlantic MIRECC. The views expressed in this article are those of the authors and do not necessarily reflect the position or policy of the Department of Veterans Affairs or the United States Government. This work was made possible with support by NIH Grants AA021697, AA021695, AA021692, AA021696, AA021681, AA021690, AA021691, and R01AG067103.

COMPETING INTERESTS

The authors declare no competing interests.

ADDITIONAL INFORMATION

Supplementary information The online version contains supplementary material available at https://doi.org/10.1038/s41386-022-01457-4.

Correspondence and requests for materials should be addressed to Rajendra A. Morey.